Self-Assembled Binary Nanoscale Systems: Multioutput Model with LFER-Covariance Perturbation Theory and an Experimental-Computational Study of NaGDC-DDAB Micelles

4 AUTHORS, INCLUDING:

Paula V Messina
Universidad Nacional del Sur
75 PUBLICATIONS   636 CITATIONS

SEE PROFILE

Humberto González-Díaz
Universidad del País Vasco / Euskal Herriko U…
230 PUBLICATIONS   6,006 CITATIONS

SEE PROFILE

Juan M. Ruso
University of Santiago de Compostela
163 PUBLICATIONS   2,044 CITATIONS

SEE PROFILE

Self-Assembled Binary Nanoscale Systems: Multioutput Model with LFER-Covariance Perturbation Theory and an Experimental–Computational Study of NaGDC-DDAB Micelles

Paula V. Messina,[†] Jose Miguel Besada-Porto,[‡] Humberto González-Díaz,[*,§,||] and Juan M. Ruso[*,‡]

[†]Department of Chemistry, INQUISUR-CONICET, Universidad Nacional del Sur, 8000 Bahía Blanca, Argentina

[‡]Soft Matter and Molecular Biophysics Group, Department of Applied Physics, University of Santiago de Compostela, Santiago de Compostela E-15782, Spain

[§]Department of Organic Chemistry II, Faculty of Science and Technology, University of the Basque Country UPV/EHU, 48940 Leioa, Spain

[||]IKERBASQUE, Basque Foundation for Science, 48011 Bilbao, Spain

ⓢ Supporting Information

ABSTRACT: Studies of the self-aggregation of binary systems are of both theoretical and practical importance. They provide an opportunity to investigate the influence of the molecular structure of the hydrophobe on the nonideality of mixing. On the other hand, linear free energy relationship (LFER) models, such as Hansch's equations, may be used to predict the properties of chemical compounds such as drugs or surfactants. However, the task becomes more difficult once we want to predict simultaneaously the effect over multiple output properties of binary systems of perturbations under multiple input experimental boundary conditions (b_j). As a consequence, we need computational chemistry or chemo-

informatics models that may help us to predict different properties of the autoaggregation process of mixed surfactants under multiple conditions. In this work, we have developed the first model that combines perturbation theory (PT) and LFER ideas. The model uses as input covariance PT operators (CPTOs). CPTOs are calculated as the difference between covariance $\Delta\mathrm{Cov}(^i\mu_k)$ functions before and after multiple perturbations in the binary system. In turn, covariances calculated as the product of two Box–Jenkins operators (BJO) operators. BJOs are used to measure the deviation of the structure of different chemical compounds from a set of molecules measured under a given subset of experimental conditions. The best CPT-LFER model found predicted the effects of 25 000 perturbations over 9 different properties of binary systems. We also reported experimental studies of different experimental properties of the binary system formed by sodium glycodeoxycholate and didodecyldimethylammonium bromide (NaGDC-DDAB). Last, we used our CPT-LFER model to carry out a 1000 data point simulation of the properties of the NaGDC-DDAB system under different conditions not studied experimentally.
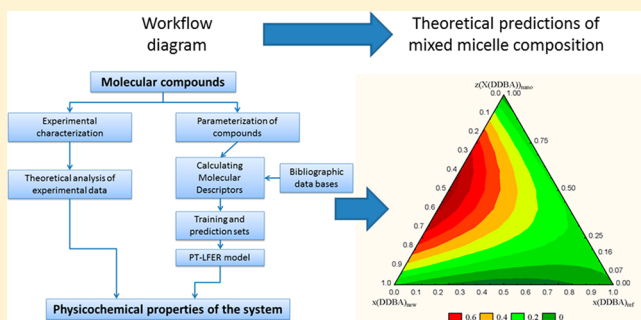
■ INTRODUCTION

Studies of the properties of mixtures of surfactants in solution are of both theoretical and practical importance. They provide an opportunity to investigate the influence of the molecular structure of the hydrophobe on the nonideality of mixing because of the wide variation in the structure of this moiety in surfactants. Several studies on the nonideality of mixing in a wide variety of different surfactant mixtures have shown a strong influence of the nature of the charge of the two molecules. Nonideal interactions, as quantified by dimensionless interaction parameter β, become progressively stronger in going from mixtures of the same surfactant type to those of opposite charge.[1,2] The magnitude of β has also been reported to be influenced by structural differences between mixed surfactants, for example, by changes in the relative hydrocarbon chain lengths of the two surfactants or changes in the

oxyethylene chain length in mixtures involving a nonionic surfactant.[3] Many biological compounds have amphiphilic behavior,[4] among them, bile salts are one of the most important. Bile salts are bile acids compounded with a cation. The bile acids contain 24 carbons, with two or three hydroxyl groups and a side chain that terminates in a carboxyl group. The carboxyl group has a pK_a of about 6; therefore, it is not fully ionized at physiological pH, hence the term bile acid. The bile acids are amphipathic in that the hydroxyl groups are α in orientation (they lie below the plane of the rings) and the methyl groups are β (they lie above the plane of the rings). Therefore, the molecules have both a polar and nonpolar

moieties and can act as emulsifying agents in the intestine, helping to prepare dietary triacylglycerol and other complex lipids for degradation by pancreatic digestive enzymes.[5−7]

On the other hand, extrathermodynamic approaches closely related to linear free energy relationships (LFER) have been successfully used in chemoinformatics.[8,9] The designation as LFER equations comes from the use of parameters depending on the Gibbs free energy (G_i) of the *i*thprocess.[10] The changes in the values of this potential during a process obey a logarithmic statistical thermodynamic relationship with equilibrium constants K_i.[11]

$$f(\varepsilon_i) = a_0 + a_1 \Delta G_i(\text{ionization}) + a_2 \Delta G_i(\text{partition}) \quad (1)$$

$$\Delta G_i = -RT \log(K_i) \quad (2)$$

$$f(\varepsilon_i) = b_0 + b_1 \log P + b_2 \, pK_a \quad (3)$$

In addition, it is known that steric, electrostatic, and hydrophobicity factors may be biologically relevant.[12−14] In fact, Corwin Hansch, one of the founders of modern chemoinformatics in the 1960s developed a LFER-like model including similar terms.[15,16] In Hansch's method, values of well-known physicochemical parameters used to approach LFER factors such as the change in free energy of the drug partitioning process, $\Delta G_i(\text{partition}) = -RT \log(P_i)$, and the change in free energy for drug ionization, $\Delta G_i(\text{partition}) = -RT \log(K_{ai})$, were used as inputs. The physicochemical parameters used more in this sense are the water/*n*-octanol partition coefficients (P) and the logarithmic acidity constants (pK_a). Hansch extended the LFER method using an extrathermodynamic approach that involves other (non-LFER) physicochemical parameters to quantify different global molecular properties such as the molecular refractivity (MR).[17] Hansch also generalized the use of lipophilicity parameters to formulate parabolic models for nonlinear relationships. Very often, log P is used as a measure of molecular lipophilicity, playing an important role in the model. We can predict log P values in turn either by atomic methods (such as X log P or A log P) or by chemical fragment methods (such as C log P or similar methods).[18−20] Also, it is possible to include other physicochemical parameters or molecular descriptors to quantify the effect of changes in chemical structural over a property of interest. This means that, for a given system, molecular descriptors can be based not only on thermodynamic parameters but also on other physicochemical properties such as lipophilicity, electronegativity, polarizability, molecular topology, and so on.

$$f(\varepsilon_i) = a_0 + a_1 \log P + a_2 pK_a + a_3 MR + a_4 \, (\log P)^2 \quad (4)$$

In general, the values of these input variables (^iV_k) may be calculated as physicochemical parameters or molecular descriptors of different types (k) for a given molecule (m_i). As a particular case, we can use as input only LFER parameters such as thermodynamic $^iV_k = {}^i\mu_k$. The outputs of the model are the values of one molecular property (ε_i) or a function of this property $f(\varepsilon_i)$ for a given chemical compound or molecular entity (m_i). In fact, we can extend the notation including general thermodynamic or extrathermodynamic functions of LFER parameters as follows.

$$f(\varepsilon_i) = \sum_{k=1}^{k_{\max}} a_k \, {}^i\mu_k + \sum_{k=1}^{k_{\max}} b_k ({}^i\mu_k)^2 + e_0 \quad (5)$$

Overall, the basic assumption for Hansch's analysis and LFER methods is that similar molecules have similar biological activities and physicochemical properties.[21−23] This means that we need to quantify small variations or perturbations in the molecular structural level that in turn should imply a small linear change in the free energy or potential of the process. In our opinion, perturbation theory (PT) ideas could be enforced to address this issue in the context of chemoinformatics applied to study complex molecular systems. To a large extent, sense perturbational methods start with a known exact solution of a problem and continue adding small terms to the mathematical description in order to approach a solution to a related problem without a known exact solution. The history of applications of PT ideas on time and system scales ranges from Copernico's astonomical model of planetary orbits in the 16th century to Bouzarth's model of micrometer-sized particle orbits to Poincaré's theory of chaos for small perturbations that can produce large nonlinear effects in a complex system (butterfly effect). PT ideas also appeared in the Bohr model of the atom, Heisenberg matrix mechanics, the Stark effect, and the Zeeman effect in the age of quantum mechanics (QM).[24−26]

We believe that PT-LFER models offer important advantages for studies involving self-aggregation and physichochemical properties of binary systems and other mixtures of surfactants and/or drugs in solution which are of both theoretical and practical importance. However, this task becomes more difficult once we want to predict simultaeously the effect of multiple input experimental conditions (b_j) over multiple output properties in binary systems. In addition, in a mixture of a drug and a surfactant we can clearly distinguish the role of each component. However, in surfactant−surfactant binary systems both molecules play indistinguishable roles. It could be possible to study each system experimentally, but the number of possible combinations of ouput properties, measured under different subsets of conditions, for many possible mixtures will detemine a very large number of experimental outcomes to be determined. As a consequence, we need computational chemistry or chemoinformatics models that may help us to predict different properties of these classes of mixtures under multiple conditions. That is why in this work we have built the first model that combines PT and LFER ideas. The model uses as input covariance PT operators (CPTOs). CPTOs are calculated as the difference in covariance $\Delta \text{Cov}(^i\mu_k)$ functions before and after multiple perturbations in the binary system. In turn, we can calculate the covariances calculated as the product of two Box−Jenkins operators (BJO) operators. BJOs are used to measure the deviation of the structure of different chemical compounds from a set of molecules measured in a given subset of experimental conditions (b_j). The best CPT-LFER model found predicted the effects of 25 000 perturbations over 9 different properties of binary systems.

Next, in the Experimental Section, we have examined the behavior and properties of mixed amphiphilic system sodium glycodeoxycholate (NaGDC)-didodecyldimethylammonium bromide (DDAB). This system not only provides a theoretical description of the involved mechanism in the heteroassembly process but also can overcome some limits on drug delivery for use in different routes of administration because of their major relevance in the design of nanosized vehicles such as liposomes

or micelles. Last, we used our CPT-LFER model to predict the properties of the system under different conditions not studied experimentally. CPT-LFER models of this type may provide an opportunity to investigate the influence of the molecular structure of the hydrophobe on the nonideality of mixing because of the wide variation in the structure of this moiety in surfactants.

■ MATERIALS AND METHODS

Experimental Section. *Experimental Materials.* Dihidroxy bile salt sodium glycodeoxycholate (NaGDC, assay ≥97%) and didodecyldimethylammonium bromide (DDAB, ≥ 98%) (Figure 1)
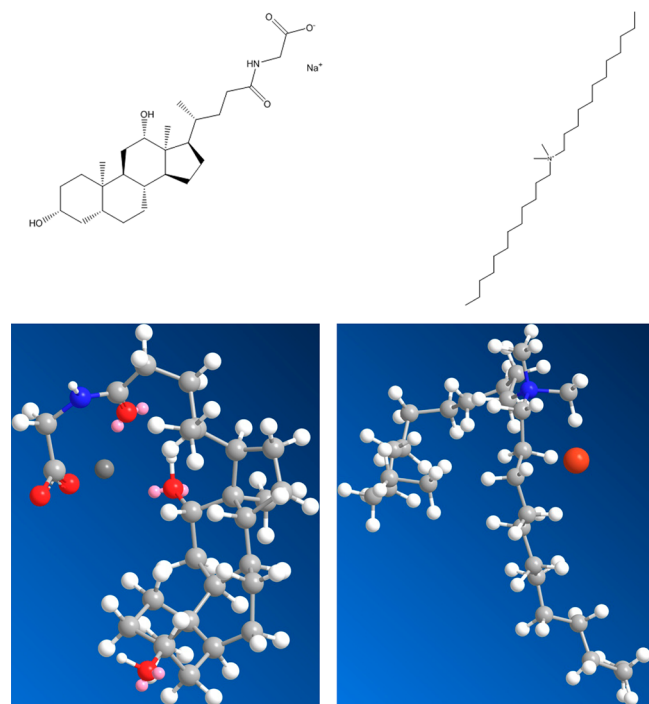

Figure 1. Top: Structural formulas of NaGDC (left) and DDAB (right). Bottom: ChemBioDraw 3D MM2 minimized model at 298 K.

were purchased from Sigma-Aldrich and used as received. Pyrene (Sigma-Aldrich, 99%) was used as a fluorescent probe. Stock NaGDC and DDAB solutions (0.1 mol dm^{-3}) were prepared and diluted as required for each experiment. The appropriate amounts of NaGDC and DDAB stock solutions were mixed to obtain the different NaGDC-DDAB mixture solutions. All surfactants and the fluorescence probe solution were prepared using double-distilled water.

Fluorescence Spectroscopy. Fluorescence spectra of pyrene were obtained with a Cary Eclipse spectrophotometer equipped with a temperature-control device and a multicell sample holder (Varian Instruments Inc.). All samples were prepared with saturated solutions of pyrene (3 × 10^{-7} mol dm^{-3}). Measurements were performed at 298 K, and the fluorescence intensities ratios (I_1/I_3) of the first (I_1, 373 nm) and third (I_3, 384 nm) peaks from the short wavelength in the spectra of pyrene were obtained with excitation at $\lambda = 335$ nm. The excitation and emission slit widths were set to be 5 and 1.5 nm, respectively.

Theoretical Section. *Workflow Used for CPT-LFER Chemo- informatics Study.* In this section we carried out a chemoinformatics study of the results obtained in the Experimental Section and other from public literature. In Figure 2, we show the workflow diagram that illustrates the integration of both sections (experimental and theoretical). The diagram briefly explains the Experimental Section to focus on the subsequent development of the CPT-LFER models. For the analysis, we started collecting the experimental values $^P\varepsilon_{ij}$ of
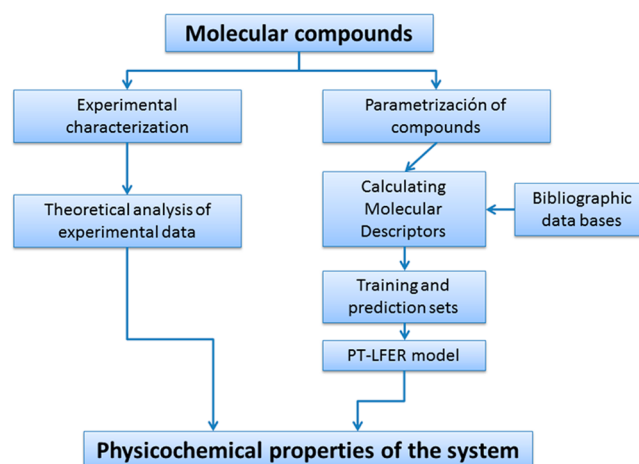

Figure 2. Workflow.

multiple properties (p) of binary systems of the surfactants that have been experimentally measured under different conditions b_j. The list of properties withdrawn from the literature includes values of the cmc (critical micellar concentration), the variation of ΔG (Gibbs potential or free energy), ΔH (enthalpy), and ΔS (entropy of the self-aggregation process) (Supporting Information). Next, we defined the CPT-LFER model. After that, we calculated the value input variables of the CPT-LFER model. These variables $^iT_k = \mathrm{Cov}(\Delta^i\mu_k)$ are covariance (Cov) functions of the different LFER extrathermodynamic potentials $^i\mu_k$ of k classes of the binary systems. After that we performed the statistical analysis and obtained the PT-LFER model. In the following text, we explain some of these steps in more detail.

Calculation of LFER Terms. The original data set contains vectors $\mathbf{v}_{ij} = [^0f(^P\varepsilon_{ij})_{ref}, \alpha_i, {}^iq_1, {}^iq_2, D_{12}, I_j, T_j]$ with the raw data inputs of this analysis. These statistical cases encoded by $\mathbf{v}_i$ vectors are perturbations of one entry or state of reference (changes in input parameters) that yield an output or new state. With the values we calculate the vectors of thermodynamic potential $\mu_{ij} = [^0f(^P\varepsilon_{ij})_{ref}, {}^i\mu_{dip}, {}^i\mu_{sol}, {}^i\mu_{part}]$. We calculated three types of LFER operators for each neutral molecule or organic ion. These operators were the thermodynamic potentials $^i\mu_k$ of type k. The types of potentials calculated were the electrostatic dipole potential $^i\mu_{dip}$ ($k = 1$), electrostatic potential in solution $^i\mu_{sol}$ ($k = 2$), and thermodynamic potential for water−nonpolar phase partitioning $^i\mu_{part}$ ($k = 3$). The formulas of the LFER potentials $^i\mu_k$ used as primary inputs are

$$^i\mu_{dip} = -q_1q_2D_{12} \tag{6}$$

$$^i\mu_{sol} = -\alpha_iq_1q_2(D_{12})^2\frac{I_j}{T_j} \tag{7}$$

$$^i\mu_{part} = -RT\log(P_i) \tag{8}$$

We calculated the values of log P variables with DRAGON software.[27−29] The structure of the molecules was uploaded to DRAGON in the form of simplified molecular input line entry (SMILE) codes. SMILE codes are very useful in managing molecular structures[30−35] and for further calculation of the molecular descriptors;[20,36] they are used by other software such as CORAL.[37−40] We used the ChemOffice software suite (https://www.cambridgesoft.com/, Cambridgesoft.com, PerkinElmer) to obtain the SMILE codes for each molecular entity.

Box−Jenkins Operators of LFER Terms. A close inspection of the covariance terms shows that they are composition-weighted products of Box−Jenkins operators (BJOs). We calculated the values $\Delta(^i\mu_k)$ of the BJOs of the thermodynamic potentials ($^i\mu_k$) to quantify the effect of deviations on the structure of one molecule m_i from the average of all molecules measured under the same set of conditions (b_j). The value $\Delta\mu_{kj}$ is the deviation of the thermodynamic or extra-

thermodynamic-like potential μ_{kj} from the average value of this magnitude $\langle \mu_k \rangle$ for one specify boundary condition c_j:

$$\Delta V_{kj} = (^i \mu_k - \langle \mu_{kj} \rangle) \tag{9}$$

$$\langle \mu_{kj} \rangle = \frac{1}{n_j} \left(\sum_{m_i \subset c_j}^{n_j} {}^i \mu_k \right) \tag{10}$$

Calculation of CTP-LFER Operators. When we expand the previous equation of the CPT-LFER model, we can note two types of input terms. The first type of input term is the function ${}^1 f(^P \varepsilon_{ij})_{ref} = \langle ^P \varepsilon_{ij} \rangle$, the average value of $^P \varepsilon_{ij}$, under conditions b_j for a given property p out of 12 different properties. It means that ${}^1 f(^P \varepsilon_{ij})_{ref}$ is a function of the expected value $\langle ^P \varepsilon_{ij} \rangle$ of the property $^P \varepsilon_{ij}$ for any system studied under the same conditions b_j. The second class of terms includes the covariance perturbation functions $\Gamma_{jp}(k)^q$ per se. In the notation $\Gamma_{jp}(k)^q$, k is the type of potential ($k = 1$ for a dipole, $k = 2$ for solution, and $k = 3$ for partitioning; previous sections). The term q is a label used to highlight the overall formal electrostatic charge of chemical species i and ii. The notation for q is $q = 0$ when both chemical species (i and ii) are molecules, $q = (+)$ when both chemical species (i and ii) are cations, and $q = (-)$ when both chemical species (i and ii) are anions. For the sake of simplicity, we never used cross covariance terms (cation−anion, molecule−cation, etc. in the analysis). The formulas of these functions are

$$\Gamma_{jp}(k)^q = \text{Cov}_{kj}(\mu_k)_{new} - \text{Cov}_{kj}(\mu_k)_{ref} \tag{11}$$

$$\Gamma_{jp}(k)^q = [(^i \mu_k - \langle \mu_{kj} \rangle) \cdot (^{ii} \mu_k - \langle \mu_{kj} \rangle)]_{new}$$
$$- [(^{i'} \mu_k - \langle \mu_{kj} \rangle) \cdot (^{ii'} \mu_k - \langle \mu_{kj} \rangle)]_{ref} \tag{12}$$

Theoretical Details of the CPT-LFER Models. Gonzalez-Díaz et al.[41] formulated a general-purpose perturbation theory (PT) method for multiple-boundary chemoinformatics problems. One possibility of this PT method is the use of linear free energy relationship (LFER) parameters as input variables. The resulting PT-LFER model can be used to study the effect of multiple perturbations in complex molecular systems with multiple components with distinguishable roles. However, the method is unable to be used in studying complex systems with multiple components (chemical species) with indistinguishable roles. Here, we propose a reformulation of this PT-LFER method in order to tackle the problem of indistinguishability of the components. The new models are expected to be able to predict the effect of multiple input perturbations over multiple output parameters in binary systems. Let there be a binary system (with two chemical species) where at least one compound must be able to dissociate, forming in total two or four ionic species. Consider also that these species undergo a process of self-aggregation into heterogeneous micelles that can reach the nanoparticle size range. In addition, once we mix the components (create the binary system), all of these particles have indistinguishable roles (we have not clearly assigned roles such as cosolvent, carrier, additive, etc.). In so doing, first we study a data set of multiple output experimental values ($^P \varepsilon_{ij}$) with different output properties (pth) of a large number of binary systems (ith). After, we analyze the effect of changes or perturbations in multiple subsets of input conditions (b_j) over the different properties $^P \varepsilon_{ij}$. The dependent variable of the model is a general multi-output function ${}^0 f(^P \varepsilon_{ij})$ useful in quantifying the experimental values of multiple properties (p) of the system in different states; the initial or reference states (r) and their respective final or new states (n) are reached by the system after a perturbation of the initial conditions. In the CPT-LFER model we are going to consider a set of multiple initial experimental conditions ${}^{ref} b_j \equiv (b_0, b_1, b_2, b_3...b_n)$ (conditions of reference) at the beginning of the process and a different or new set of conditions ${}^{new} b_j \equiv (b_0, b_1, b_2, b_3...b_n)$ at the end of the process after one or multiple perturbations (changes in these conditions). The CPT-LFER model proposed here is an additive equation with the following form:

$${}^0 f(^P \varepsilon_{ij})_{new} = a_0 + a_1 {}^1 f(\varepsilon_{ij})_{ref} + \sum_{j=1, k=2}^{j=j_{max}, k=k_{max}} a_{kj} \Gamma_{jp}(k)^q \tag{13}$$

The output variable ${}^0 f(^P \varepsilon_{ij})_{new} = z(^P \varepsilon_{ij})$ is the result of the standardization of $^P \varepsilon_{ij}$ as a z scores. The calculation of z scores is a transformation classically used to obtain outputs with average $\langle z(^P \varepsilon_{ij}) \rangle = 0$ and standard deviation $\text{SD}(z(^P \varepsilon_{ij})) = 1$. The inputs are the vectors of PT-LFER covariance functions $\Gamma_{jp}(k)^q$, and each one of these vectors represents one statistical case (ith case) out of a total of $n = 526\,789$ cases (perturbations).

■ RESULTS AND DISCUSSION

Experimental−Theoretical Study of NaGDC-DDAB Binary Micelles. Critical micelle concentration values were
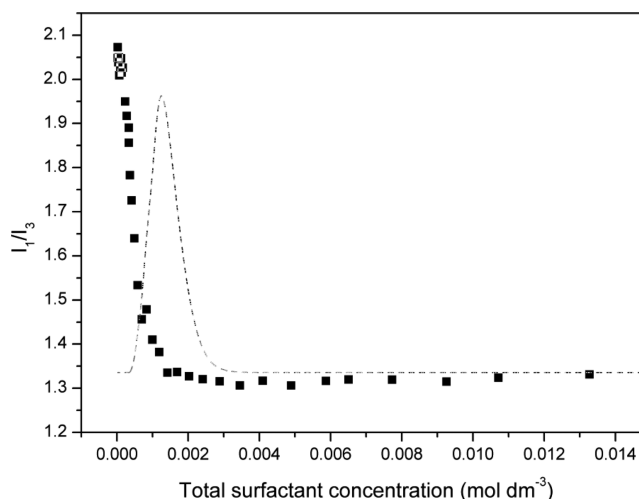

Figure 3. Fluorescence intensities ratios of the first and third vibronic picks of pyrene emission spectra (I_1/I_3) as a function of total surfactant concentration for the $\alpha_{NaGDC} = 0.3$ system. The dashed line represents the second derivative of the fluorescence−concentration curve.

Table 1. Critical Micelle Concentration, Mixed Micelle Composition, Interaction Parameter, and Gibbs Free Energy as a Function of NaGDC Molar Fraction

α_{NaGDC}	${}^{nano}cmc(mM)$	${}^{nano}x_{NaGDC}$	${}^{nano}\beta(k_B T)$	${}^{nano}\Delta G^0_m$ (kJ mol^{-1})
0	1.16			−16.74
0.1	1.06	0.29	−4.54	−16.97
0.2	0.70	0.28	−3.64	−17.99
0.3	1.21	0.34	−3.34	−16.64
0.4	2.17	0.41	−3.84	−15.19
0.5	3.51	0.51	−4.16	−14.00
0.6	3.48	0.55	−4.62	−14.02
0.7	5.74	0.69	−2.13	−12.78
0.8	5.58	0.81	−2.51	−12.85
0.9	5.61	0.87	−2.08	−12.84
1	5.90			−12.71

obtained from breaks in plots of I_1/I_3 against the total concentration of the mixture in aqueous solutions. Since there was no clear inflection point in these plots, the results were analyzed to detect a precise value of the cmc, using the Phillips definition of the critical micelle concentration, in which the cmc is defined as the concentration corresponding to the maximum change in the gradient in plots of some colligative property against total concentration. An algorithm was applied in the numerical analysis of the data that determined precise values of
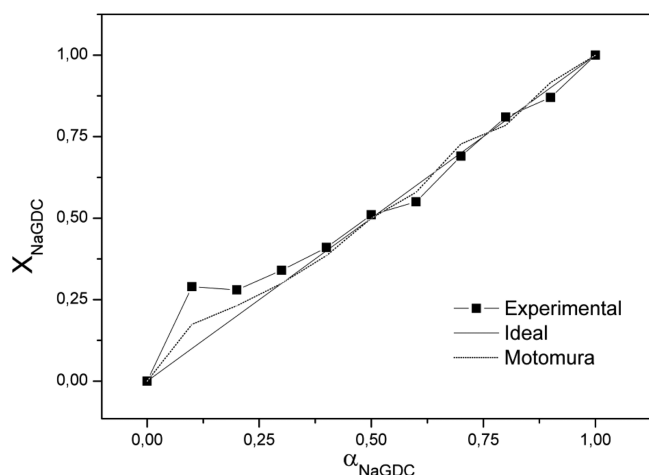
Figure 4. Plots of mixed micelle composition, X_{NaGDC}, obtained from different sources: experimental values (black squares), ideal (solid line), and Motomura (dotted line) versus total molar fraction.
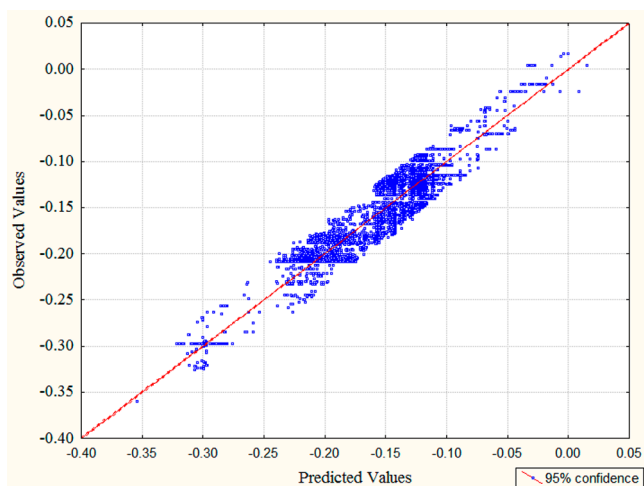

Figure 5. CPT-LFER model prediction of multiple properties of micelles (observed vs predicted values).

the critical concentrations of drugs and surfactants with low aggregation numbers. The method consists of a Gaussian approximation of the second derivative of the conductivity concentration data, followed by two consecutive numerical

integrations by the Runge−Kutta method and the Levenberg−Marquardt least-squares fitting algorithm. Figure 3 shows the maximum of the second derivative and therefore a critical micellar concentration of 1.21 mM for the $\alpha_{NaGDC} = 0.3$ system. The results obtained for all systems under study are listed in Table 1.

The composition of the mixed micelles and the changes in the distribution of the components of each system between monomeric and micellar phases have been evaluated by the analysis of the variation of the cmc with composition using different approaches. The ideal approximation of the cmc of mixed micelles as a function of composition is done with Clint's model:

$$\frac{1}{cmc_{ideal}} = \sum_i \frac{\alpha_i}{cmc_i} \tag{14}$$

This expression constitutes a relationship between the critical micellar concentration of the mixed system (cmc_{ideal}) and of the i pure components (cmc_i) and the molar fraction (α_i). However, this theory does not take into account the nonideality behavior of real mixed systems. For this reason, the composition of the monomeric and micellar phases of these systems was evaluated by the treatment of Motomura et al.[42] based on excess thermodynamic quantities, where micellization is considered to be similar to a macroscopic bulk phase and energy parameters associated with the process are expressed by excess thermodynamic quantities. The critical concentration and the mole fraction of components in the system, $\bar{x}_i$, are given by

$$cmc^* = (\nu_1 x_1 + \nu_2 x_2)cmc \tag{15}$$

$$\bar{x}_i = \frac{\nu_i x_i}{\nu_1 x_1 + \nu_2 x_2} \tag{16}$$

where x_1 and x_2 are the mole fractions of components 1 and 2 and $\nu_1 = \nu_{1,a} + \nu_{1,c}$ and $\nu_2 = \nu_{2,b} + \nu_{2,d}$; $\nu_{1,a}$ and $\nu_{1,c}$ are the numbers of cations and anions produced upon dissociation of component 1 and $\nu_{2,b}$ and $\nu_{2,d}$ are the numbers produced upon dissociation of component 2. The amphiphiles under investigation are 1:1 electrolytes with identical counterion charge, then $\nu_{1,a} = \nu_{1,c} = \nu_{2,b} = \nu_{2,d} = 1$ so $cmc^* = 2\ cmc$. The composition of the mixed micelle is determined using the relationship

Table 2. Sweep Matrix, Covariance Matrix, and Coefficients of the CPT-LFER Model

covariance	$\langle {}^P\varepsilon_{ij}\rangle_{new}$	$\Gamma_{jp}(dip)$	$\Gamma_{jp}(sol)$	$\Gamma_{jp}(part)$	$\Gamma_{jp}(sol)^-$	$\Gamma_{jp}(sol)^+$
$\langle {}^P\varepsilon_{ij}\rangle_{new}$	0.000	0.000	0.000	0.000	0.000	0.000
$\Gamma_{jp}(dip)^0$		0.000	0.000	0.000	0.000	0.000
$\Gamma_{jp}(sol)^0$			0.012	0.000	0.002	−0.014
$\Gamma_{jp}(part)^0$				0.000	0.000	0.000
$\Gamma_{jp}(sol)^-$					0.003	−0.005
$\Gamma_{jp}(sol)^+$						0.019
model	β	SE	B	SE	t	p
a_0			0.181375	0.002	108.8	0.001
$\langle {}^P\varepsilon_{ij}\rangle_{new}$	−0.458	0.002	−0.275152	0.001	−193.1	0.001
$\Gamma_{jp}(dip)^0$	−3.697	0.022	−0.158186	0.001	−166.0	0.001
$\Gamma_{jp}(sol)^0$	0.867	0.043	0.037112	0.002	20.1	0.001
$\Gamma_{jp}(part)^0$	0.411	0.002	0.017595	0.000	173.6	0.001
$\Gamma_{jp}(sol)^-$	−3.508	0.020	−0.150110	0.001	−173.9	0.001
$\Gamma_{jp}(sol)^+$	2.233	0.042	0.095564	0.002	53.7	0.001

Table 3. Average Properties of Potentials for Different Input/Output Conditions

property	$\langle \mu_{ij}(\mathrm{dip}) \rangle$	$\langle \mu_{ij}(\mathrm{sol}) \rangle$	$\langle \mu_{ij}(\mathrm{part}) \rangle$	$\langle {}^{\mathrm{P}}\varepsilon_{ij} \rangle$	$\mathrm{SD}({}^{\mathrm{P}}\varepsilon_{ij})$
β	1.14319809	0.01131703	4701.567	−0.040	6.42
cmc	1.16341030	0.01178695	5395.792	0.248	1.18
ΔG	1.16517857	0.01184776	5479.602	−14.975	7.87
X_{m1}	1.13449024	0.01029247	8892.178	0.520	0.34
X_{m2}	1.14123007	0.01077712	9978.641	0.481	0.34
A	1.00000000	0.00000916	−10 256.956	41.807	25.42
γ	1.00000000	0.00000916	−10 256.956	27.602	4.83
ΔH	1.00000000	0.00000925	−8477.038	3.336	7.53
ΔS	1.00000000	0.00000925	−8477.038	82.596	26.16
N	1.70000000	0.00005235	−13 978.519	70.300	48.14
$f1$	1.00000000	0.00065068	−9917.067	0.694	0.26
$f2$	1.00000000	0.00065068	−9917.067	0.815	0.12
counteranion	$\langle \mu_{ij}(\mathrm{dip})^{-} \rangle$	$\langle \Delta\mu_{ij}(\mathrm{sol})^{-} \rangle$	$\langle \Delta\mu_{ij}(\mathrm{part})^{-} \rangle$	SMART code	free
bromide	1.460585	0.000089	−15 223.868	[Br⁻]	yes
carboxylate	1.000000	0.000059	61 488.694	C(=O)[O⁻]	no
chloride	1.000000	0.000011	−8530.522	[Cl⁻]	yes
sulfate	1.000000	0.000009	−8318.713	S(=O)(=O)[O⁻]	no
oxide	3.718750	0.214099	−9012.713	[O⁻]	no
2-methoxyethanolate	1.000000	0.000009	−10 136.560	COCC[O⁻]	no
countercation	$\langle \mu_{ij}(\mathrm{dip})^{+} \rangle$	$\langle \mu_{ij}(\mathrm{sol})^{+} \rangle$	$\langle \mu_{ij}(\mathrm{part})^{+} \rangle$	SMART code	free
phosphine	1.000000	0.000009	−28 602.581	[P⁺]	no
sodium	1.000000	0.000038	32 631.454	[Na⁺]	yes
amine-ter	1.482998	0.038085	−11 207.204	[N⁺]	no
amine-sec	1.377358	0.000034	−10 700.483	[NH⁺]	no
	0.000000	0.000000	−10 640.488	no ionic	

$$\overline{x}_2^{\mathrm{m}} = \overline{x}_2 - \left(\frac{\overline{x}_1 \overline{x}_2}{\mathrm{cmc}^*}\right)\left(\frac{\partial \mathrm{cmc}^*}{\partial \overline{x}_2}\right)_{T,p}\left[1 - \frac{\delta_{\mathrm{d}}^{\mathrm{c}}\nu_{1,\mathrm{c}}\nu_{2,\mathrm{d}}}{\nu_{1,\mathrm{c}}\nu_2 \overline{x}_1 + \nu_{2,\mathrm{d}}\nu_1 \overline{x}_2}\right] \quad (17)$$

where $\overline{x}_i^{\mathrm{m}}$ can be expressed in a similar way to eq 17. The Kronecker delta, $\delta_{\mathrm{d}}^{\mathrm{c}}$, for systems investigated here, in which counterions are identical, is 1, and eq 17 reduces to

$$\overline{x}_2^{\mathrm{m}} = \overline{x}_2 - \left(\frac{\overline{x}_1 \overline{x}_2}{\mathrm{cmc}^*}\right)\left(\frac{\partial \mathrm{cmc}^*}{\partial \overline{x}_2}\right)_{T,p} \quad (18)$$

In Figure 4 we have plotted the experimental values of the cmc for the mixed system with the ideal approximation as a function of α_{NaGDC}. Although the different models exhibit relatively good agreement with experimental points, slight differences can be extrapolated from a visual inspect of the plots. For instance, for α_{NaGDC} values below 0.5, the Motomuràs model shows a better correlation with the experimental points. Meanwhile, for α_{NaGDC} values of up to 0.5, the behavior of the systems is almost ideal.

To gain a quantitative understanding of the mixing process, it is worth applying regular solution theory to obtain β, the dimensionless intramicellar interaction parameter, which is related to the molecular interactions in the mixed micelles and can be interpreted in terms of an energy parameter that represents the excess Gibbs free energy of mixing[1,43] $\beta = \beta_{12} = N_{\mathrm{A}}(W_{11} + W_{22} + 2W_{12})$, where W_{11} and W_{22} are the energies of interaction between molecules in the pure micelle and W_{12} is the interaction between two species in the mixed micelle. In the case of binary nonideal mixtures the regular approximation for the activity coefficients in the mixed micelles is given by

$$f_1 = \exp \beta X_2^{\,2} = \exp \beta(1 - X_1)^2 \quad (19)$$

$$f_2 = \exp \beta X_1^{\,2} \quad (20)$$

The value of β (in $k_{\mathrm{B}}T$ units) can be calculated from eq 21:

$$\frac{X_1^{\,2}\ln(\alpha_1 \mathrm{cmc_m}/(X_1 \mathrm{cmc_1}))}{(1 - X_1)^2 \ln[(1 - \alpha_1)\mathrm{cmc_m}/((1 - X_1)\mathrm{cmc_2})]} = 1 \quad (21)$$

$$\beta = \frac{\ln(\alpha_1 \mathrm{cmc_m}/(X_1 \mathrm{cmc_1}))}{(1 - X_1)^2} \quad (22)$$

In an ideal mixed micelle, β is equal to zero whereas repulsive interactions yield positive values, indicating a possible antagonism. Positive β values have been found in mixtures of fluorocarbon−hydrocarbon surfactants. Negative β values indicate attractive synergic interactions which imply that the $\mathrm{cmc_m}$ is lower that the averaged value of the cmc of each surfactant. Although theoretically β is independent of the temperature and composition of the micelles, some papers show a temperature dependence and also a micelle composition dependence.[44,45] Table 1 listed the mixed micelle composition and the interaction parameter, respectively, as a function of bile salt concentration by applying the RST. β indicates the nature and strength of the interaction between both amphiphilic molecules, which means that it is a measure of the degree of nonideality in mixed micelles, i.e., a negative value of β is associated with a stronger attractive interaction between the two different molecules.[46] On the other hand, positive values yield repulsive interactions. Table 1 shows interaction parameter β over the complete range of NaGDC molar fraction, and the tendency of this parameter increases with the molar fraction of bile salts. This fact highlights the great synergism between sodium glycodeoxycholate and didodecyl-dimethylammonium bromide. Finally, it can be concluded that the mixed system formed by NaGDC and DDAB exhibits a

Table 4. Selected Results of 1000-Point Simulation of an NaGDC/DDBA Micelle Nanoparticle Binary System

system	micelle nanosystem				Γ_{pjk}				
$x(DDBA)_{ref}$	$x(DDBA)_{new}$	$z(cmc)_{nano}$	$z(x(DDBA))_{nano}$	$z(\Delta G)$	$k = dip$	$k = sol$	$k = part$	$q < 0$	$q > 0$
0.00	0.10	−0.27	−0.23	−0.27	−0.55	−0.44	0.34	0.89	−0.39
	0.30	−0.46	−0.33	−0.46	−0.87	−0.81	−0.27	1.60	−0.70
	0.50	−0.48	−0.33	−0.48	−1.22	−1.18	−0.88	1.53	−1.04
	0.70	−0.43	−0.26	−0.43	−1.59	−1.57	−1.52	1.10	−1.41
	1.00	−0.20	−0.21	−0.17	−2.08	−2.11	−2.43	0.68	−1.96
0.30	0.10	−0.02	0.05	0.01	−0.55	−0.43	0.34	−0.98	−0.45
	0.30	−0.15	−0.06	−0.15	−0.90	−0.80	−0.28	−0.27	−0.77
	0.50	−0.20	−0.05	−0.21	−1.24	−1.18	−0.90	−0.34	−1.11
	0.70	−0.18	−0.02	−0.24	−1.30	−1.44	−1.38	−0.77	−1.37
	0.90	0.00	0.03	−0.09	−1.65	−1.81	−2.00	−1.14	−1.74
	1.00	0.11	0.04	0.02	−1.82	−2.00	−2.31	−1.18	−1.93
0.50	0.10	−0.08	0.10	0.06	−0.55	−0.41	0.34	−1.36	−0.48
	0.30	−0.09	0.00	−0.24	−0.90	−0.78	−0.28	−0.65	−0.81
	0.50	−0.30	0.00	−0.18	−1.22	−1.15	−0.88	−0.72	−1.14
	0.70	−0.13	0.07	−0.10	−1.59	−1.53	−1.52	−1.15	−1.51
	0.90	0.05	0.09	−0.10	−1.65	−1.80	−2.00	−1.53	−1.78
	1.00	0.17	0.12	0.16	−2.10	−2.09	−2.45	−1.57	−2.07
0.70	0.10	0.02	0.05	−0.02	−0.53	−0.38	0.35	−1.05	−0.51
	0.30	−0.14	−0.05	−0.15	−0.90	−0.77	−0.28	−0.35	−0.85
	0.50	−0.36	−0.07	−0.23	−0.96	−1.04	−0.76	−0.42	−1.09
	0.70	−0.31	−0.01	−0.18	−1.30	−1.42	−1.38	−0.85	−1.44
	0.90	0.00	0.07	−0.03	−1.93	−1.88	−2.14	−1.22	−1.92
	1.00	−0.04	0.07	−0.04	−2.10	−2.07	−2.45	−1.26	−2.11
0.90	0.10	−0.14	−0.12	−0.20	−0.27	−0.27	0.48	−0.06	−0.46
	0.30	−0.29	−0.23	−0.35	−0.61	−0.65	−0.14	0.64	−0.78
	0.50	−0.41	−0.20	−0.41	−1.24	−1.12	−0.90	0.57	−1.22
	0.70	−0.30	−0.14	−0.33	−1.56	−1.48	−1.50	0.15	−1.57
	0.90	−0.15	−0.09	−0.18	−1.91	−1.85	−2.12	−0.23	−1.94
	1.00	−0.09	−0.08	−0.07	−2.08	−2.03	−2.43	−0.27	−2.13
1.00	0.10	−0.25	−0.21	−0.25	−0.55	−0.36	0.34	0.69	−0.58
	0.30	−0.35	−0.32	−0.36	−0.90	−0.73	−0.28	1.40	−0.90
	0.50	−0.41	−0.31	−0.41	−1.22	−1.10	−0.88	1.33	−1.23
	0.70	−0.41	−0.25	−0.42	−1.56	−1.47	−1.50	0.90	−1.59
	0.90	−0.21	−0.20	−0.27	−1.93	−1.85	−2.14	0.53	−1.97
	1.00	−0.15	−0.20	−0.10	−2.08	−2.02	−2.43	0.49	−2.15

higher contribution of the bile salt in the mixed micelle, a relatively low deviation from ideal behavior, and a strong interaction of the compound in the complex (large negative interaction parameter) due to the screening of the Coulomb repulsion which enhances the complex constitution.

CPT-LFER Model for Multiple Self-Aggregation Properties of Binary Systems. In the previous section we reported the experimental determination of multiple physicochemical properties of self-aggregation in binary systems. In this work, we also collected a large data set of physicochemical properties of these systems. In our review we noted that the researchers used multiple properties to characterize these systems, measured under many diverse experimental conditions. In so doing the authors need to used different apparatus and also use theoretical models to infer the properties from experimental results. In this sense, we decided to develop by the first time one unified multioutput model able to predict all of these properties with a single equation. The CPT-LFER proposed here is able to predict with reasonable accuracy the value of multiple output properties of the system obtained after changes of the chemical structure of the two components of the system and their respective contra-ions (Figure 5), if any, as well as perturbations in other experimental boundary

conditions. The conditions considered include c_0 (output property, selected out of x total properties), c_1 (first component), c_2 (composition of the first component), c_1 (cation of first component), c_1 (contra-anion of first component), c_3 (second component), c_4 (composition of second component), c_5 (cation of second component), c_6 (contra-anion of second component), c_7 (solvent), c_8 (temperature), and c_8 (ionic strength). The best CPT-LFER model found with this algorithm was the following (details in Table 2)

$${}^0f\left({}^P\varepsilon_{ij}\right)_{new} = -0.275152\,{}^1f\left({}^P\varepsilon_{ij}\right)_{ref} - 0.158186\,\Gamma_{pj}\left(dip\right)^0$$
$$+ 0.037112\,\Gamma_{pj}\left(solv\right)^0 + 0.017595\,\Gamma_{pj}\left(part\right)^0 - 0.150110\,\Gamma_{pj}\left(solv\right)^-$$
$$+ 0.095564\,\Gamma_{pj}\left(solv\right)^+ + 0.181375$$

$N = 25\,000,\ R = 0.93,\ F = 25\,840.0,\ p < 0.001,\ SEE = 0.01595$

(23)

where the output function ${}^0f({}^P\varepsilon_{ij})_{new}$ is a multi-output function that quantifies the numerical values (ε) of different pth physicochemical properties of the ith binary system that have been experimentally determined under a certain set of jth boundary conditions (c_j). The output function used was the z score ${}^0f({}^P\varepsilon_{ij})_{new} = z({}^P\varepsilon_{ij})_{new} = ({}^P\varepsilon_{ij} - \langle {}^P\varepsilon_{ij}\rangle)/SD({}^P\varepsilon_{ij})_{new}$. The z
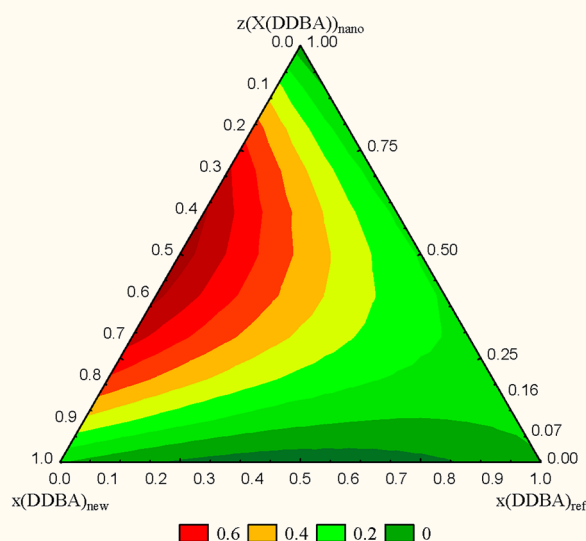
Figure 6. Ternary diagram of $z(dG)$ of formation of NaGDC-DDBA binary micelle nanoparticles for changes in the composition of micelles $z(x(\text{DDBA}))_{\text{nano}}$ after perturbations in initial composition $^{\text{new}}\alpha_{\text{DDBA}}$ vs $^{\text{ref}}\alpha_{\text{DDBA}}$ values.

score is an excellent multiscale function because it is dimensionless with average = 0 and SD = 1 for the set of values of the same property (p). The statistical parameters used were the regression coefficient of the training series (R), the Fisher ratio (Sn), the probability of error or the p level (p), and the regression coefficient of the leave-one-out validation (q^2). This new model predicts (with $R = 0.93$) the effects over 12 different experimental properties of thousands of changes or perturbations ($N = 25\,000$) under the initial conditions (b_j)

CPT-LFER Simulation of Perturbations in an NaGDC-DDAB Micelle Nanoparticle System. We are going to illustrate the use of PT-LFER methodology with a numerical simulation. In so doing, we studied the effect of perturbations over the formation of self-assembled micelle nanoparticles in a binary system. For this study we selected precisely the NaGDC-DDAB system studied in the previous section. In this section we shall predict the effect of perturbations under the initial experimental conditions over multiple physicochemical properties of the system. We need to substitute the values of the potentials of the molecules as well as the average values of the functions in the equation in order to use the model. In Table 3, we depict the values of the average functions for different properties.

We begin the simulation by generating 1000 perturbations in the system at random. This means that we selected at random 1000 pairs of new states vs their states of reference. We selected only states with perturbations in the composition of the initial system and final micelle nanoparticles. We measured the variations in composition in terms of molar fractions α_{DDBA} vs α_{NaGDC}. As these compositions are fixed, $\alpha_{\text{NaGDC}} = 1 - \alpha_{\text{DDBA}}$, we focused only on α_{DDBA} values. Other state functions were keep constant: $T = 298$ K, $I = 1$, and so forth. The 1000 perturbations generated at random included changes in initial values of $^{\text{ref}}\alpha_{\text{DDBA}}$ to obtain new values $^{\text{new}}\alpha_{\text{DDBA}}$ in the full range of 0−1. After that, we calculated the values of the input LFER-covariance functions $(\Gamma_{pj}(\text{dip})^0, \Gamma_{pj}(\text{part})^0, \Gamma_{pj}(\text{sol})^0, \Gamma_{pj}(\text{sol})^-$, and $\Gamma_{pj}(\text{sol})^+)$ for all these pairs of values using the average values in Table 3. Next, we introduced the values in the

CPT-LFER model and predicted the perturbations in multiple properties of the system. In Table 4, we summarize only some of the results of the 1000-point simulation for these 3 properties of the micelle nanoparticles.

The three output properties summarized in Table 4 are the critical micelle concentration (cmc), composition of DDBA in the final micelle nanoparticles $^{\text{nano}}\alpha_{\text{DDBA}}$, and variations in the Gibbs free energy of formation of the micelle ΔG. We also carried out a ternary diagram graphical analysis of the results of the simulation. In Figure 6, we depicted graphically the ternary diagram for the analysis of the CPT-QSPR model simulation of NaGDC-DDBA binary micelle nanoparticles. The variable depicted in the color scale is the z score of the free energy of formation of the micelle nanoparticles $z(\Delta G)_{\text{nano}}$. Variable $z(\Delta G)_{\text{nano}} > 0$ when the predicted free energy ΔG is lower than $\langle \Delta G \rangle$, the expected or average free energy. We should take into consideration in this data set all of the values of $\Delta G < 0$. Consequently, the higher values of $z(\Delta G)_{\text{nano}}$ indicate the formation of more stable micelle nanoparticles. In this sense, the use of the present model may be useful in predicting multiple properties and constructing the ternary systems of binary systems of bile salts toward the computational design of more stable micelle nanoparticles.

CONCLUSIONS

In this work the physicochemical properties of the nanoparticles spontaneously formed within aqueous mixtures of bile salts sodium glycodeoxycholate and surfactant didodecyldimethylammonium bromide (NaGDC-DDAB) as a function of its concentration are investigated by a combined experimental/computational study. The experimental study has been carried out by means of a thermodynamic analysis and fluorescence spectroscopy experiments. Regarding the theoretical study, the models of Clint and Motomura have been used to predict the monomeric and micellar compositions. On the other hand, we also present a new computational method for predicting these key physicochemical properties including the free energy, critical micellar concentration or intramicellar interaction. For this purpose we have developed the first model which combines perturbation theory (PT) and linear free energy relationship (LFER) ideas. We clearly show that a single model may have a good quality of predicting multiple properties. Results obtained by our model were compared with published data, and our experimental results obtained standard errors of estimates of less than 0.02%. We have also predicted results for our system under different conditions that were not experimentally studied. The detailed analysis and theoretical model provided in the present work is expected to be useful as a reference to design in a fast and economical way new nanoparticles based on surfactant mixtures.

ASSOCIATED CONTENT

Ⓢ Supporting Information

The Supporting Information is available free of charge on the ACS Publications website at DOI: 10.1021/acs.langmuir.5b03074.

Name, structure (SMILE codes), and some parameters of the compounds (PDF)

AUTHOR INFORMATION

Corresponding Authors

*E-mail: humberto.gonzalezdiaz@ehu.es.

*E-mail: juanm.ruso@usc.es.

Notes

The authors declare no competing financial interest.

■ REFERENCES

(1) Blanco, E.; Verdes, P. V.; Ruso, J. M.; Prieto, G.; Sarmiento, F. Interactions in binary mixed systems involving betablockers with different lipophilicity as a function of temperature and mixed ratios. *Colloids Surf., A* **2009**, *334*, 116−123.

(2) López-Fontán, J. L.; Blanco, E.; Ruso, J. M.; Prieto, G.; Schulz, P. C.; Sarmiento, F. The aqueous catanionic system sodium perfluorooctanoate−dodecyltrimethylammonium bromide at low concentration. *J. Colloid Interface Sci.* **2007**, *312*, 425−431.

(3) Holland, P. M. Modeling Mixed Surfactant Systems: Basic Introduction. In *Mixed Surfactant Systems*; Holland, P. M., Rubingh, D. N., Eds.; American Chemical Society: 1992; Vol. *501*, pp 31−44.

(4) Ruso, J. M.; Deo, N.; Somasundaran, P. Complexation between Dodecyl Sulfate Surfactant and Zein Protein in Solution. *Langmuir* **2004**, *20*, 8988−8991.

(5) Hofmann, A. F.; Small, D. M. Detergent Properties of Bile Salts: Correlation with Physiological Function. *Annu. Rev. Med.* **1967**, *18*, 333−376.

(6) Fernández-Leyes, M.; Verdinelli, V.; Hassan, N.; Ruso, J.; Pieroni, O.; Schulz, P.; Messina, P. Biomimetic formation of crystalline bone-like apatite layers on spongy materials templated by bile salts aggregates. *J. Mater. Sci.* **2012**, *47*, 2837−2844.

(7) Messina, P. V.; Prieto, G.; Ruso, J. M.; Fernández-Leyes, M. D.; Schulz, P. C.; Sarmiento, F. Thermodynamic and elastic fluctuation analysis of langmuir mixed monolayers composed by dehydrocholic acid (HDHC) and didodecyldimethylammonium bromide (DDAB). *Colloids Surf., B* **2010**, *75*, 34−41.

(8) Roy, K.; Leonard, J. T. QSAR analyses of 3-(4-benzylpiperidin-1-yl)-N-phenylpropylamine derivatives as potent CCR5 antagonists. *J. Chem. Inf. Model.* **2005**, *45*, 1352−68.

(9) Anslyn, E. E.; Dougherty, D. A. *Modern Physical Organic Chemistry*; University Science Books: 2006; p 455.

(10) Gibbs, J. W. *A Method of Geometrical Representation of the Thermodynamic Properties of Substances by Means of Surfaces*; The Academy: 1871.

(11) Greiner, W.; Rischke, D.; Neise, L.; Stöcker, H. *Thermodynamics and Statistical Mechanics*; Springer: New York, 2000.

(12) Chaudhaery, S. S.; Roy, K. K.; Saxena, A. K. Consensus Superiority of the Pharmacophore-Based Alignment, Over Maximum Common Substructure (MCS): 3D-QSAR Studies on Carbamates as Acetylcholinesterase Inhibitors. *J. Chem. Inf. Model.* **2009**, *49*, 1590−601.

(13) Chou, K. C.; Cai, Y. D. Prediction of membrane protein types by incorporating amphipathic effects. *J. Chem. Inf. Model.* **2005**, *45*, 407−13.

(14) Estrada, E.; Uriarte, E.; Molina, E.; Simon-Manso, Y.; Milne, G. W. An integrated in silico analysis of drug-binding to human serum albumin. *J. Chem. Inf. Model.* **2006**, *46*, 2709−24.

(15) Hansch, C.; Steward, A. R.; Iwasa, J. The Correlation of Localization Rates of Benzeneboronic Acids in Brain and Tumor Tissue with Substituent Constants. *Mol. Pharmacol.* **1965**, *1*, 87−92.

(16) Kubinyi, H. *QSAR: Hansch Analysis and Related Approaches*; VCH Publishers: Weinheim, 1993; Vol. *1*.

(17) Ehresmann, B.; de Groot, M. J.; Clark, T. Surface-integral QSPR models: local energy properties. *J. Chem. Inf. Model.* **2005**, *45*, 1053−60.

(18) Tetko, I. V.; Poda, G. I. Application of ALOGPS 2.1 to predict log D distribution coefficient for Pfizer proprietary compounds. *J. Med. Chem.* **2004**, *47*, 5601−4.

(19) Eros, D.; Kovesdi, I.; Orfi, L.; Takacs-Novak, K.; Acsady, G.; Keri, G. Reliability of logP predictions based on calculated molecular descriptors: a critical review. *Curr. Med. Chem.* **2002**, *9*, 1819−29.

(20) Tetko, I. V.; Tanchuk, V. Y.; Kasheva, T. N.; Villa, A. E. Internet software for the calculation of the lipophilicity and aqueous solubility of chemical compounds. *J. Chem. Inf. Model.* **2001**, *41*, 246−52.

(21) Hansch, C.; Hoekman, D.; Leo, A.; Weininger, D.; Selassie, C. D. Chem-bioinformatics: comparative QSAR at the interface between chemistry and biology. *Chem. Rev.* **2002**, *102*, 783−812.

(22) Hansch, C.; Kurup, A.; Garg, R.; Gao, H. Chem-bioinformatics and QSAR: a review of QSAR lacking positive hydrophobic terms. *Chem. Rev.* **2001**, *101*, 619−72.

(23) Hansch, C.; Steinmetz, W. E.; Leo, A. J.; Mekapati, S. B.; Kurup, A.; Hoekman, D. On the role of polarizability in chemical-biological interactions. *J. Chem. Inf. Model.* **2003**, *43*, 120−5.

(24) Poincaré, H. Sur le problème des trois corps et les équations de la dynamique. *Acta Mathematica* **1890**, *13*, 1−270.

(25) Bouzarth, E. L.; Brooks, A.; Camassa, R.; Jing, H.; Leiterman, T. J.; McLaughlin, R. M.; Superfine, R.; Toledo, J.; Vicci, L. Epicyclic orbits in a viscous fluid about a precessing rod: theory and experiments at the micro- and macro-scales. *Phys. Rev. E* **2007**, *76*, 016313.

(26) Cropper, W. H. *Great Physicists: The Life and Times of Leading Physicists from Galileo to Hawking*; Oxford University Press, 2004; p 512.

(27) Helguera, A. M.; Combes, R. D.; Pérez González, M.; Cordeiro, M. N. D. S. Applications of 2D descriptors in drug design: A DRAGON tale. *Curr. Top. Med. Chem.* **2008**, *8*, 1628−1655.

(28) Papa, E.; Villa, F.; Gramatica, P. Statistically validated QSARs, based on theoretical descriptors, for modeling aquatic toxicity of organic chemicals in Pimephales promelas (fathead minnow). *J. Chem. Inf. Model.* **2005**, *45*, 1256−66.

(29) Mauri, A.; Consonni, V.; Pavan, M.; Todeschini, R. DRAGON Software: An Easy Approach to Molecular Descriptor Calculations. *MATCH* **2006**, *56*, 237−248.

(30) Toropov, A. A.; Toropova, A. P.; Benfenati, E.; Leszczynska, D.; Leszczynski, J. SMILES-based optimal descriptors: QSAR analysis of fullerene-based HIV-1 PR inhibitors by means of balance of correlations. *J. Comput. Chem.* **2010**, *31*, 381−92.

(31) Toropov, A. A.; Benfenati, E. SMILES as an alternative to the graph in QSAR modelling of bee toxicity. *Comput. Biol. Chem.* **2007**, *31*, 57−60.

(32) Toropov, A. A.; Benfenati, E. SMILES in QSPR/QSAR Modeling: results and perspectives. *Curr. Drug Discovery Technol.* **2007**, *4*, 77−116.

(33) Karwath, A.; De Raedt, L. SMIREP: predicting chemical activity from SMILES. *J. Chem. Inf. Model.* **2006**, *46*, 2432−44.

(34) Siani, M. A.; Weininger, D.; Blaney, J. M. CHUCKLES: a method for representing and searching peptide and peptoid sequences on both monomer and atomic levels. *J. Chem. Inf. Model.* **1994**, *34*, 588−93.

(35) Siani, M. A.; Weininger, D.; James, C. A.; Blaney, J. M. CHORTLES: a method for representing oligomeric and template-based mixtures. *J. Chem. Inf. Model.* **1995**, *35*, 1026−33.

(36) Vidal, D.; Thormann, M.; Pons, M. LINGO, an efficient holographic text based method to calculate biophysical properties and intermolecular similarities. *J. Chem. Inf. Model.* **2005**, *45*, 386−93.

(37) Miteva, M. A.; Violas, S.; Montes, M.; Gomez, D.; Tuffery, P.; Villoutreix, B. O. FAF-Drugs: free ADME/tox filtering of compound collections. *Nucleic Acids Res.* **2006**, *34*, W738−44.

(38) Toropova, A. P.; Toropov, A. A.; Benfenati, E.; Gini, G.; Leszczynska, D.; Leszczynski, J. CORAL: quantitative structure-activity relationship models for estimating toxicity of organic compounds in rats. *J. Comput. Chem.* **2011**, *32*, 2727−33.

(39) Toropova, A. P.; Toropov, A. A.; Benfenati, E.; Gini, G.; Leszczynska, D.; Leszczynski, J. CORAL: QSPR models for solubility

of [C60] and [C70] fullerene derivatives. *Mol. Diversity* **2011**, *15*, 249−56.

(40) Toropov, A. A.; Toropova, A. P.; Rasulev, B. F.; Benfenati, E.; Gini, G.; Leszczynska, D.; Leszczynski, J. CORAL: QSPR modeling of rate constants of reactions between organic aromatic pollutants and hydroxyl radical. *J. Comput. Chem.* **2012**, *33*, 1902−6.

(41) Gonzalez-Diaz, H.; Arrasate, S.; Gomez-SanJuan, A.; Sotomayor, N.; Lete, E.; Besada-Porto, L.; Ruso, J. M. General theory for multiple input-output perturbations in complex molecular systems. 1. Linear QSPR electronegativity models in physical, organic, and medicinal chemistry. *Curr. Top. Med. Chem.* **2013**, *13*, 1713−41.

(42) Motomura, K.; Yamanaka, M.; Aratono, M. Thermodynamic consideration of the mixed micelle of surfactants. *Colloid Polym. Sci.* **1984**, *262*, 948−955.

(43) Blanco, E.; Messina, P.; Ruso, J. M.; Prieto, G.; Sarmiento, F. Regarding the Effect that Different Hydrocarbon/Fluorocarbon Surfactant Mixtures Have on Their Complexation with HSA. *J. Phys. Chem. B* **2006**, *110*, 11369−11376.

(44) Crisantino, R.; De Lisi, R.; Milioto, S. Energetics of sodium dodecylsulfate-dodecyldimethylamine oxide mixed micelle formation. *J. Solution Chem.* **1994**, *23*, 639−662.

(45) Treiner, C.; Khodja, A. A.; Fromon, M. Micellar solubilization of 1-pentanol in binary surfactant solutions: a regular solution approach. *Langmuir* **1987**, *3*, 729−735.

(46) Shiloach, A.; Blankschtein, D. Predicting Micellar Solution Properties of Binary Surfactant Mixtures. *Langmuir* **1998**, *14*, 1618−1636.